


Sensitivity of Antarctic sea ice to the Southern Annular Mode in coupled climate models

Marika M. Holland¹  · Laura Landrum¹ · Yavor Kostov² · John Marshall²

Received: 30 June 2016 / Accepted: 22 October 2016
© Springer-Verlag Berlin Heidelberg 2016

Abstract We assess the sea ice response to Southern Annular Mode (SAM) anomalies for pre-industrial control simulations from the Coupled Model Intercomparison Project (CMIP5). Consistent with work by Ferreira et al. (J Clim 28:1206–1226, 2015. doi:10.1175/JCLI-D-14-00313.1), the models generally simulate a two-timescale response to positive SAM anomalies, with an initial increase in ice followed by an eventual sea ice decline. However, the models differ in the cross-over time at which the change in ice response occurs, in the overall magnitude of the response, and in the spatial distribution of the response. Late twentieth century Antarctic sea ice trends in CMIP5 simulations are related in part to different modeled responses to SAM variability acting on different time-varying transient SAM conditions. This explains a significant fraction of the spread in simulated late twentieth century southern hemisphere sea ice extent trends across the model simulations. Applying the modeled sea ice response to SAM variability but driven by the observed record of SAM suggests that variations in the austral summer SAM, which has exhibited a significant positive trend, have driven a modest sea ice decrease. However, additional work is needed to narrow the considerable model uncertainty in the climate response to SAM variability and its implications for 20th–21st century trends.

Keywords Antarctic sea ice · Southern Annular Mode · Climate models

✉ Marika M. Holland
mholland@ucar.edu

¹ NCAR, Boulder, CO, USA

² MIT, Cambridge, MA, USA

1 Introduction

Since the 1970s, a dramatic reduction in stratospheric ozone over Antarctica has occurred in response to chlorofluorocarbon emissions. Associated with this ozone depletion is a poleward shift and strengthening of the surface westerlies associated with the mid-latitude jet of the southern hemisphere (e.g. Thompson and Wallace 2000). This occurs primarily in late spring and summer and projects onto the positive polarity of the Southern Annular Mode (SAM), which exhibits a positive trend over the late twentieth century in the December to February seasonal mean (e.g. Marshall 2003). These SAM trends have the ability to influence Antarctic surface climate through wind-forcing of the Southern Ocean. For example, evidence from the historical record suggests that SAM variability is related to variations in sea ice (e.g. Stammerjohn et al. 2008; Pezza et al. 2012; Simpkins et al. 2012) and surface temperatures (e.g. Kwok and Comiso 2002; Thompson and Solomon 2002) among other properties.

Model simulations indicate that in response to a positive SAM, increased northward surface Ekman drift occurs with enhanced downwelling near 45S and upwelling near the Antarctic continent (Hall and Visbeck 2002; Lefebvre et al. 2004). Relationships determined from interannual variability suggest a dipole-like response in sea ice area to SAM variations, with positive anomalies in the Ross Sea region and negative anomalies along the Antarctic peninsula that extend into the Atlantic (e.g. Lefebvre et al. 2004). This pattern bears some similarity to the observed long-term sea ice trends, leading to the speculation that SAM trends are in part responsible. The increases in observed total Antarctic sea ice extent are seemingly consistent with modeling work that suggests that the total Antarctic sea ice cover increases following a positive SAM anomaly (e.g. Hall and Visbeck

2002; Sen Gupta and England 2006). However several other modeling studies seem to contradict these results and suggest that sea ice extent declines in response to a positive SAM anomaly induced from ozone loss (e.g. Sigmond and Fyfe 2010; Bitz and Polvani 2012; Smith et al. 2012).

Ferreira et al. (2015) reconciled these various studies by showing that the modeled Antarctic sea surface temperature and sea ice exhibit a two-timescale response to SAM variations. This includes a fast response in which a positive SAM anomaly and associated enhanced westerlies lead to increased equatorward Ekman transport in the ocean surface and sea ice. This increases the sea ice cover both dynamically, due to direct wind forcing, and thermodynamically, due to colder sea surface temperatures (SSTs). On longer timescales, the deeper ocean circulation responds to the changes in wind forcing leading to increased upwelling of deeper and warmer ocean waters. This provides a thermodynamic forcing to the sea ice and leads to reduced ice growth and/or enhanced melting. As such, the sea ice extent anomalies associated with a positive SAM exhibit an increase in the short term but a decrease on longer timescales.

The presence of this two-timescale response has been explicitly documented in two different models that apply an abrupt loss of stratospheric ozone (Ferreira et al. 2015). Questions remain however on how robust these relationships are within climate models, including the magnitude of the sea ice response, the timescales associated with the fast and slow response, and the switch-over from cooling to warming. Additionally, the simulations discussed in Ferreira et al. (2015) and other related previous work (Sigmond and Fyfe 2010; Bitz and Polvani 2012) were subject to abrupt changes in ozone. Work using twentieth century single forcing ozone experiments (Sigmond and Fyfe 2014) provide insights on the transient response to ozone loss and support a general decrease in ice associated with transient ozone loss. However, uncertainties remain in the mechanisms relating SAM forcing to sea ice conditions during the late twentieth–early 21st century. Finally, while some studies have documented regional variations in SAM-driven sea ice conditions (Lefebvre et al. 2004; Stammerjohn et al. 2008), little work has been done to diagnose how these differ across models and on longer timescales. Given that the twentieth century sea ice trends have large regional variations, it is useful to consider possible spatial variations in the sea ice response to SAM for longer timescales and across multiple models.

Here, we explore these issues by assessing the relationships between SAM and sea ice variability in a large number of Coupled Model Intercomparison Project 5 (CMIP5; Taylor et al. 2012) models. A complementary paper (Kostov et al. 2016) provides an assessment for sea surface temperatures within the Southern Ocean. Our analysis includes

the influence of SAM variability on both the total hemispheric and regional sea ice in pre-industrial control simulations at various timescales. We also consider whether the relationships derived from these unforced pre-industrial runs can explain some aspects of sea ice trends, and their across-model scatter, within the twentieth century.

2 Model simulations

Our analysis makes use of the pre-industrial (Table 1) and twentieth century (Table 2) simulations from 29 different CMIP5 models. We assess multiple twentieth century ensemble members for individual CMIP5 models, where available. These calculations come from multiple modeling centers and generally have differences across the model components. As noted by Knutti et al. (2013) however, some of the models are not strictly independent. We do assume independence when computing the significance of results and as such, the significance of some of our results may be overstated.

Our analysis also makes use of a large ensemble of simulations performed with the Community Earth System Model (referred to as CESM-LE; Kay et al. 2015), which uses the CESM-CAM5 model (Hurrell et al. 2013; note that this is also one of the CMIP5 models). The CESM-LE encompasses 40 members for the 1920–2100 time period and a 2000 year pre-industrial control run. The twentieth century members differ only in a round-off level perturbation in their initial 1920 atmospheric state and so any difference in their simulation is purely due to the model's internal variability.

3 Pre-industrial control runs analysis

We assess CMIP5 pre-industrial (PI) control runs as listed in Table 1. As shown, the timeseries length is different across the various models. For our analysis, we use the longest timeseries possible from the different simulations. A number have sizable sea ice extent trends over the length of the PI timeseries indicating that they are not well equilibrated (Table 1; see also Turner et al. 2013a). We remove a linear trend from the ice extent timeseries prior to analysis. This may be problematic in some cases given that the equilibration may not be linear. In general though, it does not qualitatively affect the results.

The annual cycle of pre-industrial southern hemisphere ice extent from the collection of CMIP5 simulations is shown in Fig. 1. As is clear, and noted in other studies (e.g. Turner et al. 2013a, 2015; Shu et al. 2015), the models differ considerably in their simulation of the mean Antarctic sea ice cover. Indeed considerable biases exist in climate model

Table 1 Models used in the analysis. The short name is used to designate the various models on figures

Model name	Short name	PI model years/timeseries length	Max/min/mean ice extent	Ice extent trend
ACCESS1-0	A	300–549/250	2.1/20.0/11.8	–0.21
ACCESS1–3	B	250–749/500	5.6/21.0/14.2	0.11
Bcc-csm1-1	C	1–500/500	3.9/25.0/16.5	0.04
CanESM2	D	2015–3110/1095	4.4/24.2/14.6	0.07
CCSM4	E	800–1300/500	11.6/25.4/20.2	0.10
CESM1-WACCM	F	96–295/200	8.2/21.4/16.4	–0.19
CESM1-CAM5	G	1–319/319	6.4/21.4/15.5	–0.08
CMCC-CESM	H	4324–4600/277	2.7/22.3/12.7	0.10
CMCC-CM	I	1550–1819/270	3.5/21.3/13.0	0.02
CMCC-CMS	J	3684–4183/500	2.7/21.9/12.7	–0.07
CNRM-CM5	K	1850–2699/850	0.1/19.2/9.4	–0.11
CSIRO-Mk3-6-0	L	1–500/500	9.6/21.1/15.9	–0.07
EC-EARTH	M	2100–2551/451	2.5/19.8/11.5	0.05
GISS-E2-H	N	2410–2949/540	0.9/11.0/6.2	–0.27
GFDL-CM3	O	1–500/500	0.4/13.3/7.0	–0.49
GFDL-ESM2G	P	1–500/500	0.9/15.7/8.7	–0.05
GFDL-ESM2 M	Q	1–500/500	0.2/13.3/7.1	–0.09
HadGEM2-CC	R	1860–2099/240	2.2/16.7/9.6	0.05
Inmcm4	S	1850–2349/500	1.3/13.1/7.2	0.07
IPSL-CM5A-LR	T	1800–2799/1000	1.1/21.8/11.1	–0.08
IPSL-CM5A-MR	U	1800–2099/300	0.4/18.3/8.6	–0.17
IPSL-CM5B-LR	V	1830–2129/300	0.1/10.1/4.3	–0.31
MIROC5	W	2000–2699/700	0.2/7.1/3.5	–0.24
MIROC-ESM	X	1800–2330/531	2.9/22.3/13.6	–1.04
MIROC-ESM-CHEM	Y	1850–2100/251	3.6/24.2/15.0	–0.82
MPI-ESM-LR	Z	1850–2849/1000	1.5/17.6/8.6	0.01
MPI-ESM-MR	a	1850–2849/1000	1.3/18.0/8.9	0.01
MRI-CGCM3	b	1851–2350/500	3.9/19.5/13.0	–0.03
NorESM1-M	c	700–1200/500	5.6/19.9/13.6	–0.11

The ice model metrics are computed for the pre-industrial control simulations and ice extent values are shown in 10^6 km². Ice extent trends are for annual mean values and are in units of 10^6 km² per century

simulations of the Southern Ocean more generally. For example, the models differ greatly in numerous Southern Ocean properties including, the atmospheric energy budgets (Previdi et al. 2015), cloud conditions (Hwang and Frierson 2013), surface air temperature (Schneider and Reusch 2016), and ocean properties (e.g. Downes and Hogg 2013; Sallée et al. 2013) among others. In terms of sea ice, the simulations exhibit considerable internal variability with a typically red spectrum. The characteristics of simulated internal variability differ across the models, as is clear from the monthly standard deviation of ice extent (Fig. 1b). Differences extend to other variability metrics as well.

In addition to total southern hemisphere ice extent, we assess regional characteristics of ice area. This regional ice variability is analyzed using the timeseries of ice area as a function of longitude. The simulated ice area is computed for 5-degree longitude sectors around the Antarctic

continent for comparison. The ice area regional mean and standard deviation for the various models is shown in Fig. 2 and indicates that, for these properties, there is also considerable across-model scatter. The models also differ from observations. Most notably, all of the CMIP5 models simulate larger winter and spring variability in total ice extent (Fig. 1b) than is present in observations. Although this comparison is between pre-industrial climate simulations and observations, a similar discrepancy is found when analyzing present-day conditions from the climate models as has been previously noted by Zunz et al. (2013). The large modeled ice extent variability is primarily due to discrepancies in ice area variability in the Weddell Sea region (Fig. 2b) and also a lack of a regional compensation of sea ice area anomalies in some models when compared to observations. This is a further indication of the challenges involved in simulating the Southern Ocean and as noted by

Table 2 Information on the twentieth century CMIP5 simulations used in the analysis

Model name	Number of members	Ozone forcing
ACCESS1-0	2	P (Cionni et al. 2011)
ACCESS1-3	3	P (Cionni et al. 2011)
Bcc-csm1-1	3	P (Cionni et al. 2011)
CanESM2	5	P (Cionni et al. 2011)
CCSM4	6	P (Lamarque et al. 2011)
CESM1-WACCM	1	Interactive
CESM1-CAM5	2	P (Lamarque et al. 2011)
CMCC-CESM	1	
CMCC-CM	1	P (Cionni et al. 2011)
CMCC-CMS	1	
CNRM-CM5	5	Interactive
CSIRO-Mk3-6-0	8	P (Cionni et al. 2011)
EC-EARTH	5	P (Cionni et al. 2011)
GISS-E2-H	2	P (Hansen et al. 2007)
GFDL-CM3	5	Interactive
GFDL-ESM2G	1	P (Cionni et al. 2011)
GFDL-ESM2 M	1	P (Cionni et al. 2011)
HadGEM2-CC	1	P (Cionni et al. 2011)
Inmcm4	1	P (Cionni et al. 2011)
IPSL-CM5A-LR	5	P (Szopa et al. 2013)
IPSL-CM5A-MR	3	P (Szopa et al. 2013)
IPSL-CM5B-LR	1	P (Szopa et al. 2013)
MIROC5	5	P (Kawase et al. 2011)
MIROC-ESM	3	P (Kawase et al. 2011)
MIROC-ESM-CHEM	1	Interactive
MPI-ESM-LR	3	P (Cionni et al. 2011)
MPI-ESM-MR	3	P (Cionni et al. 2011)
MRI-CGCM3	3	P (Cionni et al. 2011)
NorESM1-M	3	P (Lamarque et al. 2011)
CESM-LE	40	P (Marsh et al. 2013)

Zunz et al. (2013) may limit the utility of the models for understanding observed sea ice variability and trends.

Following on previous work (e.g. Hall and Visbeck 2002; Lefebvre et al. 2004; Sen Gupta and England 2006), we investigate the relationship of sea ice to variability in the SAM. Here we define a SAM index as the principal component of the first empirical orthogonal function (EOF) of sea level pressure (SLP) for 20–90S (following Thompson and Wallace 2000). To compute the SAM index we use the Climate Variability Diagnostic Package described in Phillips et al. (2014). The principal component timeseries from the respective models is normalized such that a one unit SAM variation denotes a one-sigma change. We assess sea ice relationships with both an annual mean SAM index and

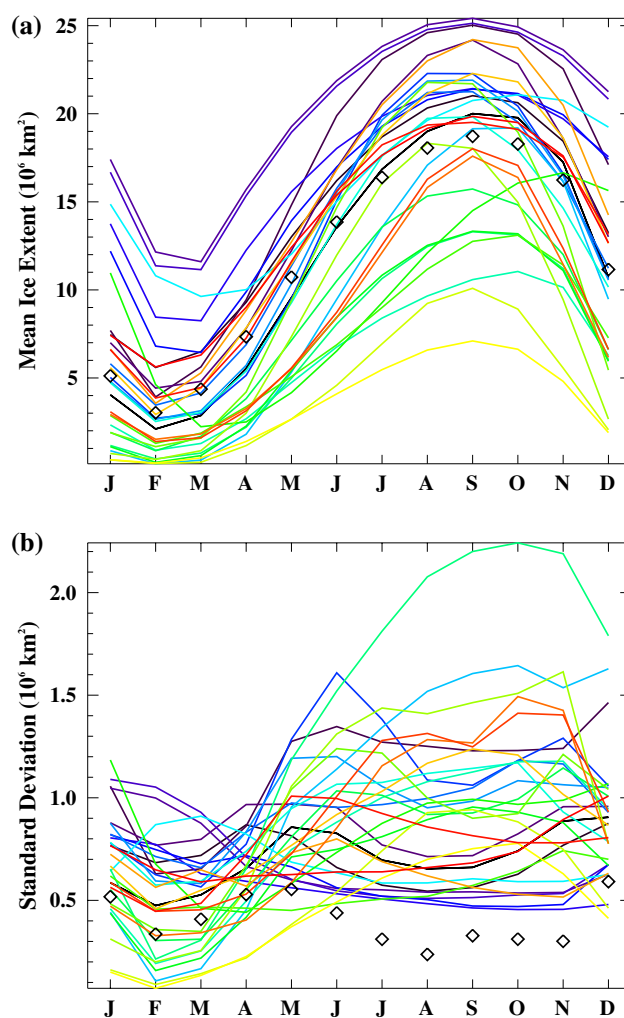


Fig. 1 The **a** mean and **b** standard deviation of monthly Antarctic sea ice extent from pre-industrial control simulations of the CMIP5 models listed in Table 1. The color legend for the various models can be found on Fig. 4. The 1979–2012 average from satellite observations (Fetterer et al. 2002) are denoted by the diamonds

an austral summer (DJF) index. The austral summer analysis is used because that is the time period that is influenced by ozone loss and exhibits SAM trends in the late twentieth century. As with sea ice metrics, the simulation of SAM variability differs across the models both in the spatial pattern of SAM anomalies and characteristics of the SAM time-series. For example, as shown in Fig. 3 for several illustrative models, some simulate considerable regional asymmetry in SAM-related SLP anomalies whereas others have a more zonal structure. The location of maximum SAM-related SLP gradients, and hence zonal wind anomalies, also differs across the models. This is consistent with previous work (Raphael and Holland 2006; Swart et al. 2015) that has assessed SAM variability within CMIP5 and other models.

To assess the relationship between sea ice and SAM variations, we use the method of Kostov et al. (2016), which

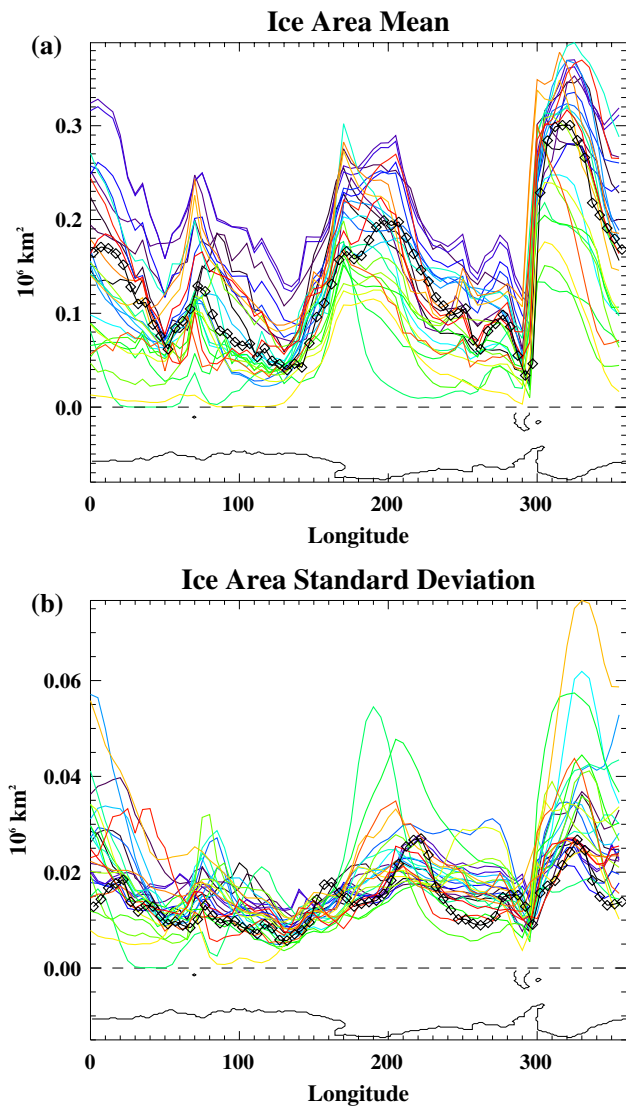


Fig. 2 The CMIP5 pre-industrial control simulation **a** mean and **b** standard deviation of the annual mean Antarctic sea ice area in 5° longitude sectors as a function of longitude. Satellite observed values (Comiso 2000) for 1979–2006 are shown by the diamonds. The horizontal dashed line indicates zero sea ice area. The continental outline of Antarctica is shown at the bottom of the plots for reference

was applied to the sea surface temperature (SST) response to SAM variability. This method assumes that the sea ice response to SAM forcing can be estimated from the convolution of an impulse response function with a previous history of time-varying SAM anomalies (see also Hasselmann et al. 1993). This is estimated for a discrete timeseries as:

$$SI(t) = \sum_{i=0}^I G(\tau_i) SAM(t - \tau_i) \Delta\tau + \varepsilon, \quad \text{with } \tau_I = \tau_{max} \quad (1)$$

where SI is the estimated sea ice variable response at time t , ε is residual noise, τ_i is the time lag which is cut off at

some maximum value τ_{max} (set to 20 years), and $\Delta\tau$ is the time interval which is equal to one year. $G(\tau_i)$ is the impulse response function (a quasi Green's function) of sea ice following an impulse perturbation of the SAM index. It is estimated using a linear least-squares regression of the sea ice variable against the lagged SAM index such that $G(\tau_i)$ equals the regression coefficient of a sea ice variable on the SAM index at a time lag of τ_i .

To assess the sea ice response (SI) to a one-sigma step change in the SAM, Eq. (1) is solved subject to a SAM value of one (e.g. $SAM(t - \tau_i) = 1$) and hence the $G(\tau_i)$ values are just summed over the τ time lags. We refer to this as the “step function response”. This analysis is done separately for each of the CMIP5 models using the entire length of the pre-industrial control simulation timeseries, resulting in a different estimated SI for each model. For sea ice variables, we assess the response function for both the total southern hemisphere sea ice extent and the longitude-dependent sea ice area. More information on the method of analysis and error estimates is available in Kostov et al. (2016).

The step function response of the total annual mean southern hemisphere sea ice extent to annual SAM anomalies is shown in Fig. 4a. All the models except for two (models F and E) tend to simulate an expansion of sea ice during a year with a positive SAM perturbation (the zero lag response shown in Fig. 4b). If monthly ice extent anomalies and the DJF SAM are considered (not shown), all models (including F and E) simulate increased sea ice extent within the months following an austral summer (DJF) SAM perturbation. This increase in sea ice is consistent with an increased equatorward Ekman transport due to enhanced westerly winds. This is identified by Ferreira et al. (2015) as the fast timescale response. Here we diagnose the SAM westerly wind response in the models from the maximum gradient in the zonal mean SAM-related SLP anomalies. Differences in the SAM-related westerly wind strength are significantly correlated ($R = 0.46$) to the magnitude of the initial annual sea ice extent increase. This indicates that models with stronger SAM related westerly wind anomalies tend to have a larger initial ice increase.

At a five year time lag, just over half of the models simulate a decrease in annual Antarctic ice extent associated with a positive step change in the SAM (Fig. 4c). At lags longer than 10 years, over 70% of the models simulate a loss of sea ice extent associated with a positive SAM (Fig. 5a). About 25% of the models never exhibit a transition from ice gain to ice loss. In general, models which have an earlier cross-over time have a greater propensity to lose ice at a given time lag. The simulated loss of sea ice extent at longer timescales agrees with the long timescale response identified in Ferreira et al. (2015) which is related to increased vertical ocean heat transport in ice covered

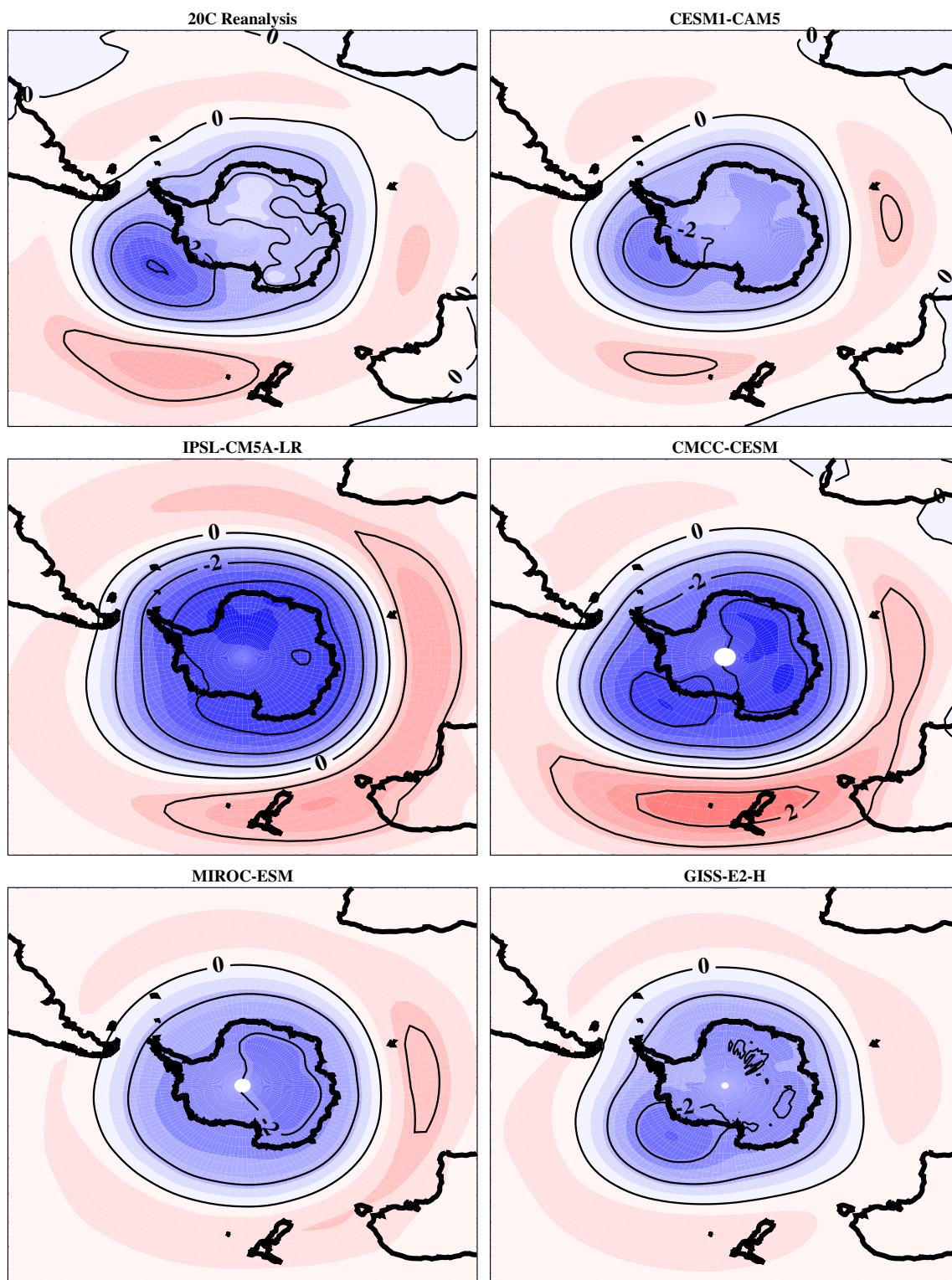
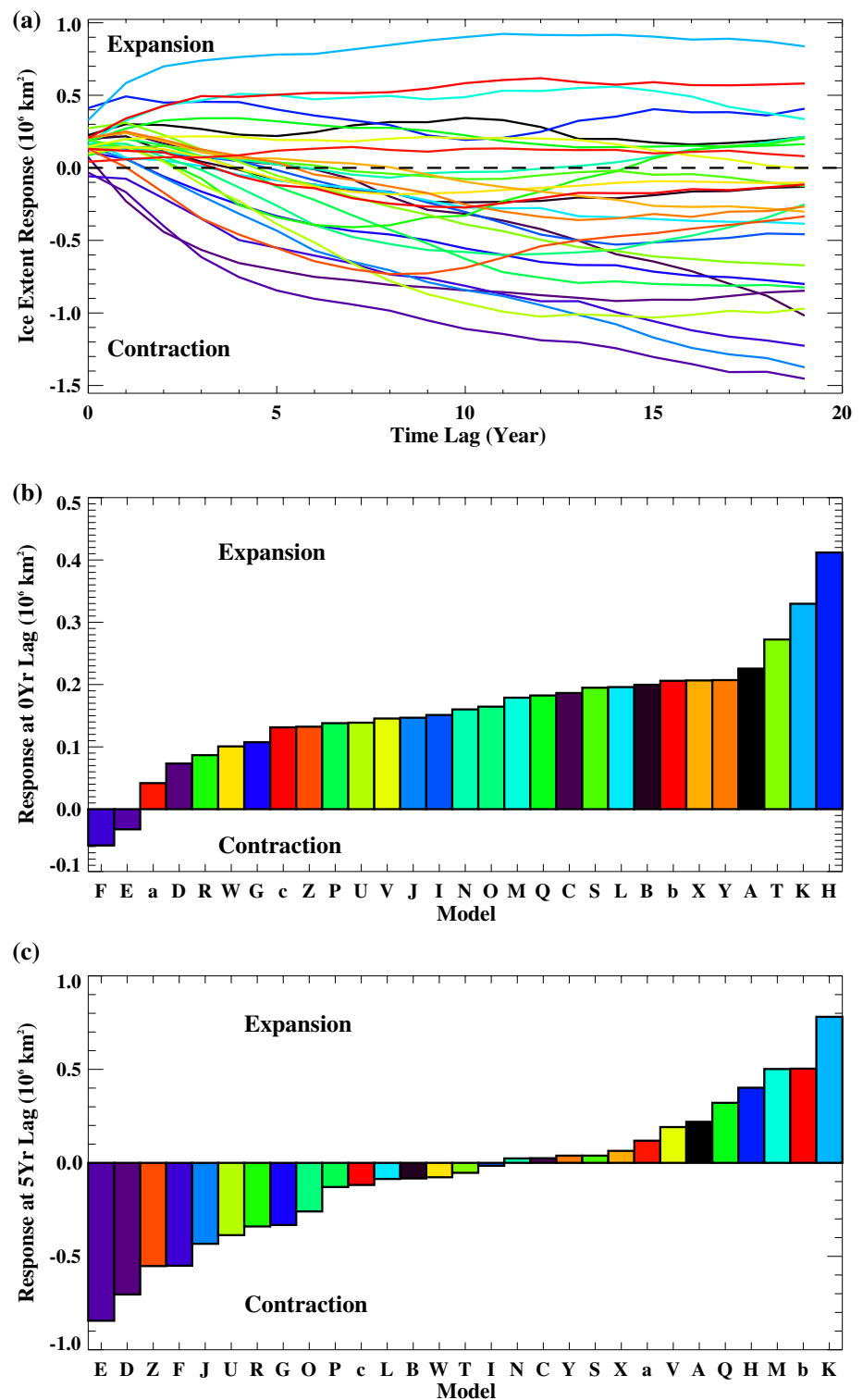


Fig. 3 The SAM SLP pattern from annual mean data for the observationally-based twentieth century reanalysis (Compo et al. 2011) for 1979–2012 (*upper left*) and pre-industrial control simulations from a

number of CMIP5 models. The spatial pattern is obtained by regressing SLP anomalies onto the normalized principal component time-series. The *solid lines* are in a contour interval of one hPa

Fig. 4 **a** The response of the total annual mean southern hemisphere sea ice extent to a one-sigma step perturbation in the annual mean SAM for the CMIP5 models analyzed. The values are shown as a function of time lag in years where the ice lags the SAM. **b** The step response in year 0 across the various CMIP5 models. **c** The step response in year 5 across the various CMIP5 models. Note that in panels **b** and **c**, the model values are shown in increasing order. The colors on the two panels indicate different models with the models designated on the x-axis. The colors for different models are consistent across the panels and for different figures. A key is provided in Table 1 enabling individual models to be identified



regions. However, the magnitude of this low-frequency sea ice response (e.g. Fig. 4c) and the timescale at which the models transition from a positive to a negative sea ice response (Fig. 5b) differs considerably across the models. This is in general agreement with the results for SST anomalies shown by Kostov et al. (2016) for a somewhat

different subset of models. Indeed, if the 21 models which are common to both studies are considered, the ice and SST step function responses are significantly correlated at all time lags. For example, at the 5-year time lag, they are correlated at $R = -0.81$ indicating that models with a tendency to lose ice following a positive SAM anomaly also

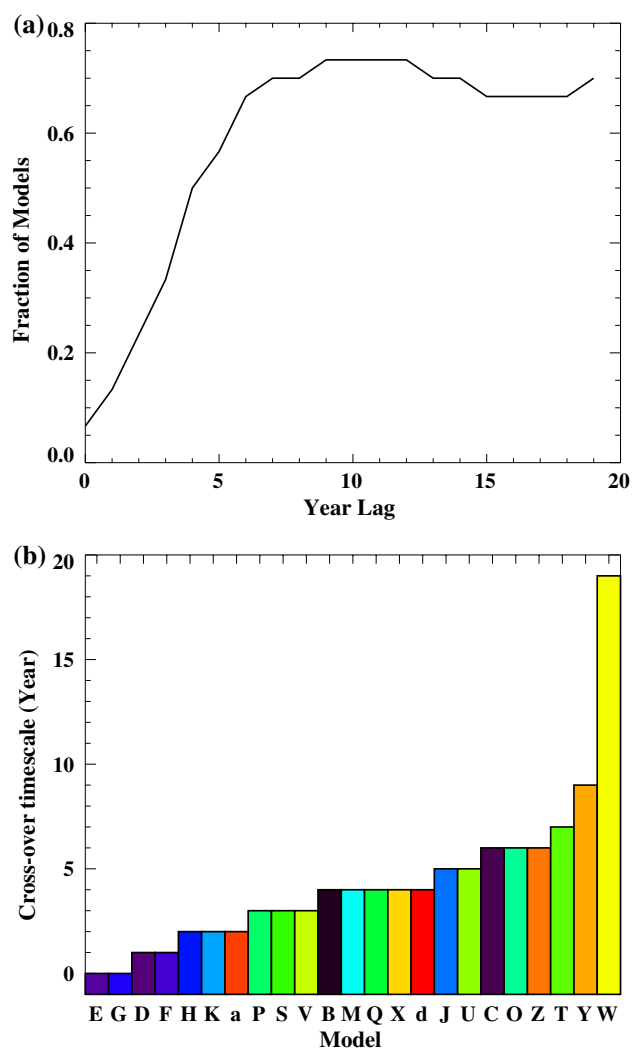


Fig. 5 **a** The fraction of the 29 analyzed models which exhibit a decrease in the response of total annual Antarctic sea ice extent to a one sigma step increase in SAM as a function of time lag and **b** the first year at which the different models transition from increased sea ice to decreased sea ice extent in response to a step increase in the SAM. In **b** the seven models which maintain an increase in sea ice for all time lags are not shown. These models include MPI-ESM-MR, ACCESS1-0, GFDL-ESM2M, CMCC-CESM, MRI-CGCM3, EC-EARTH, CNRM-CM5

have a propensity for SAM-induced surface warming. As compared to the sea ice extent response, where the majority of models transition from ice expansion to ice contraction following the SAM, fewer of the models exhibit an actual crossover in the SST response from cooling at short timescales to warming at longer timescales. This may be related to the different region associated with the analysis as the SST is averaged from 55–70S and includes areas north of the ice edge. As discussed by Kostov et al. (2016), some of the discrepancies across the models in their SAM response are associated with different mean ocean conditions, which

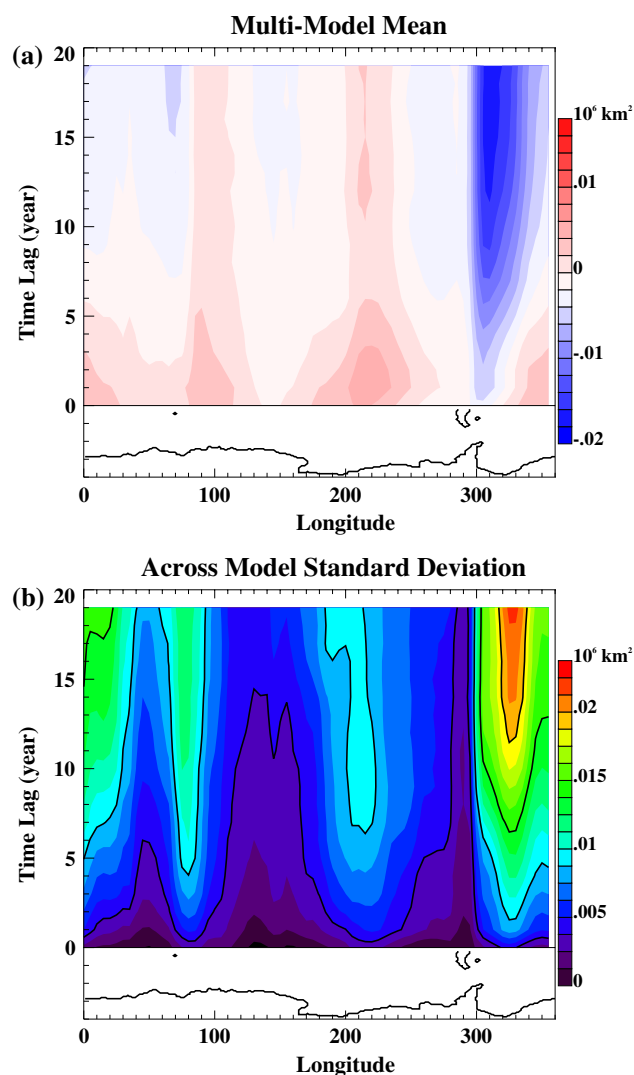


Fig. 6 Metrics of the longitude-dependent annual mean ice area response to a one sigma step increase in the annual mean SAM including, the **a** CMIP5 multi-model mean ice area response and **b** across-model standard deviation in the ice area response. Values are shown as a function of longitude and time lag. The continental outline of Antarctica is shown on the *bottom* of the figure for reference. In **a** red colors indicate expansion of ice and blue colors indicate contraction

influence how wind anomalies modify ocean heat transport. As indicated by the high correlation between the ice and SST step function response, mean ocean simulation biases almost certainly also affect the sea ice extent response within these models.

The sea ice step function response to a SAM perturbation is not spatially uniform but varies with longitude (Fig. 6). At short timescales, in the multi-model mean, ice area increases around most of the Antarctic continent except near the Antarctic Peninsula. The increases are largest around 220E in the Pacific sector. Some aspects of the

spatial character of the sea ice area response are retained for all timescales. For 200–240E, increases in sea ice are present in the multi-model mean at all time lags analyzed, although this differs across the individual models. At longer timescales, the Weddell Sea region exhibits the largest multi-model mean ice loss associated with the SAM but also the largest across-model uncertainty. The ice response in the Weddell Sea is significantly correlated to the total ice extent response, indicating that this region is a large contributor to the total ice extent step function response at longer timescales (Fig. 7).

The spatial structure of the ice response to a SAM perturbation is associated with the non-zonal character of SAM anomalies. In observations and many models, SAM anomalies project onto variability in the Amundsen Sea Low (ASL), which is a climatological feature in the region between the Antarctic Peninsula and the Ross Sea (for more information on the ASL see Fogt et al. 2012 and Turner et al. 2013b). This leads to anomalous local meridional winds, with enhanced northward winds in the Ross and Amundsen Sea and enhanced southward winds in the Bellingshausen and Weddell Seas. These anomalous winds modify ice, ocean, and atmospheric transport and affect the spatial distribution of the sea ice area response. The models differ in their simulation of these non-annular aspects of the SAM and are typically more annular than the observationally-based reanalysis data (Fig. 8a), although this may be influenced by the different length of the timeseries available. To quantify the non-annular SAM variations, we assess the departures of the SAM-related SLP anomalies from their respective zonal means within each model at 60S (Fig. 8a). This is interpolated to a 5-degree longitude grid for consistency. A measure of the non-annular component of the SAM is computed as the standard deviation of these SLP anomalies with longitude. This metric is strongly related to the strength of the low SLP anomalies that are associated with the ASL and to the associated anomalous geostrophic meridional winds.

Differences across the models in the spatial pattern of sea ice response are significantly correlated to this metric of the non-annular component of the SAM (Fig. 8b). Models with a less annular SAM tend to exhibit increased ice in the Ross and Amundsen Sea and reduced ice near the Antarctic peninsula immediately following a SAM anomaly. Significant correlations are also retained within the Pacific sector for longer timescales, with negative correlations emerging in the western Ross Sea at a 5-year time lag. This analysis suggests that the meridional component of the SAM-associated winds, which are related to the ASL variation, is important for the resulting spatial structure of sea ice anomalies. This has some consistency to observed relationships between sea ice and SAM variability (Fig. 8c), which indicates similar regional sea ice anomalies associated

with SAM variations on interannual timescales. This suggests that those models with a less annular SAM structure may exhibit a more realistic sea ice response on short timescales. However, within the models, this has little impact on the total southern hemisphere sea ice extent, because in models with a stronger projection of SAM anomalies onto the ASL and hence a less zonal structure, both enhanced northerly and southerly winds occur and lead to compensating sea ice area anomalies.

4 Twentieth century simulations

4.1 SAM and sea ice conditions

Over the late twentieth century, significant increases in the SAM have been observed in austral summer. This is associated with reductions in stratospheric ozone caused by the use of chlorofluorocarbons (CFCs) and to a lesser extent, with rising greenhouse gases (e.g. Arblaster and Meehl 2006; Thompson et al. 2011). Here we consider twentieth century climate model simulations that prescribe historical forcings, including greenhouse gases, volcanic emissions, solar variability at the top of the atmosphere, and ozone concentrations. For the stratospheric ozone changes, the models either prescribe or simulate ozone based on the observed record, although the datasets and time evolution of ozone change can differ among the models (Table 2). Eyring et al. (2013) further discuss the ozone changes within the CMIP5 models and some associated impacts. Here we consider whether simulated changes in the DJF SAM during the twentieth century, which are affected by ozone loss, can influence Antarctic sea ice trends within the climate models.

Climate models suggest that there is considerable internal variability due to the chaotic nature of the climate system even on multi-decadal timescales (e.g. Deser et al. 2012). This is true for many climate metrics and modes of variability, including the SAM. For example, Fig. 9a shows multi-decadal DJF SAM trends from the CESM-CAM5 Large Ensemble (CESM-LE; Kay et al. 2015) simulations for the pre-industrial and twentieth century climates. In the twentieth century, the CESM-LE runs use prescribed ozone as calculated by a high-top coupled chemistry–climate model (Marsh et al. 2013). This ozone forcing agrees well with observations. The simulations also apply time-varying greenhouse gas concentrations, volcanic emissions, and solar variability at the top of the atmosphere based on the historical record. The differences among the twentieth century runs from the CESM-LE are purely attributable to simulated internal variability as all runs use the same model and same forcing and only differ slightly at a round-off level perturbation in their initial state in 1920.

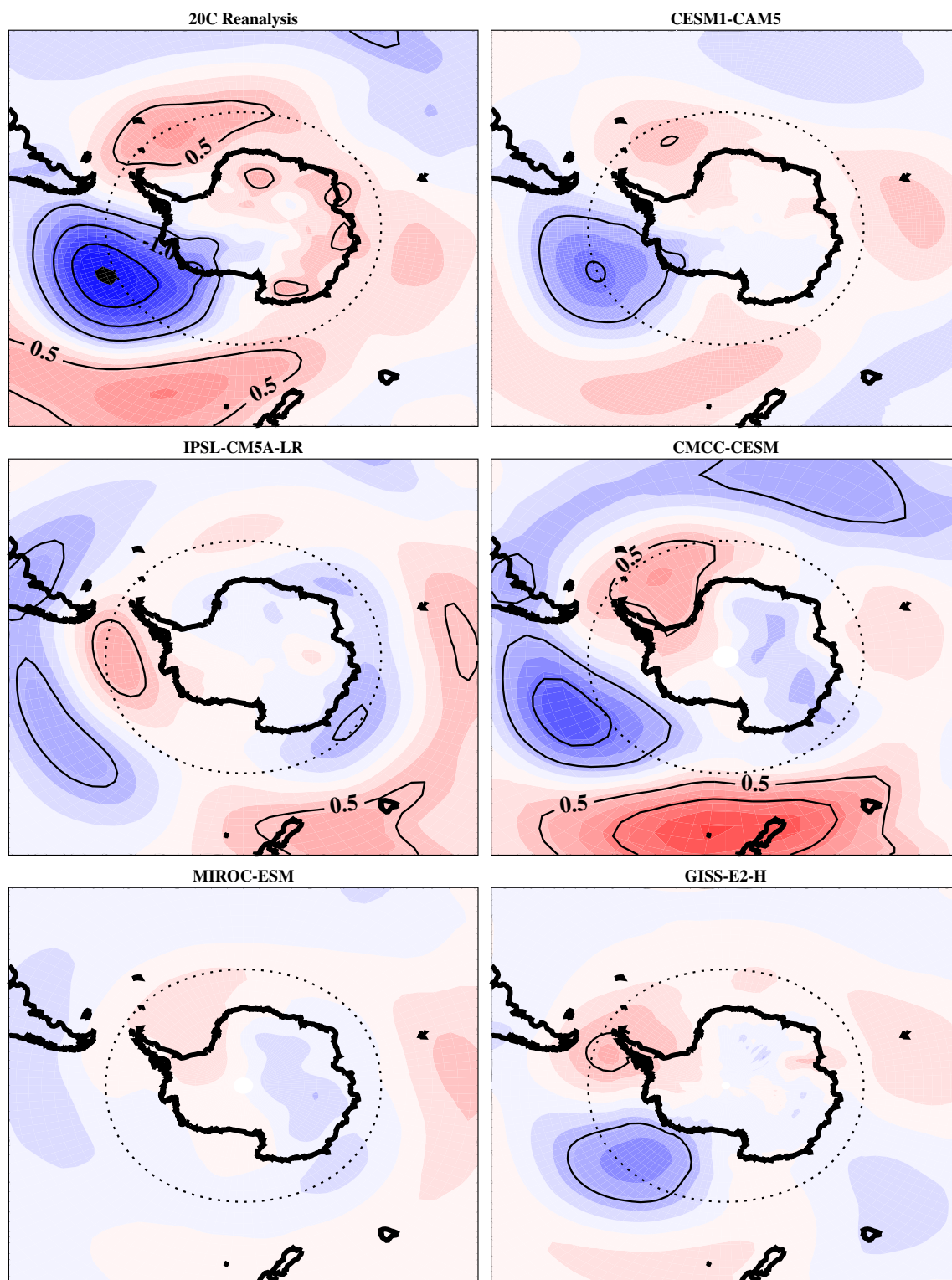
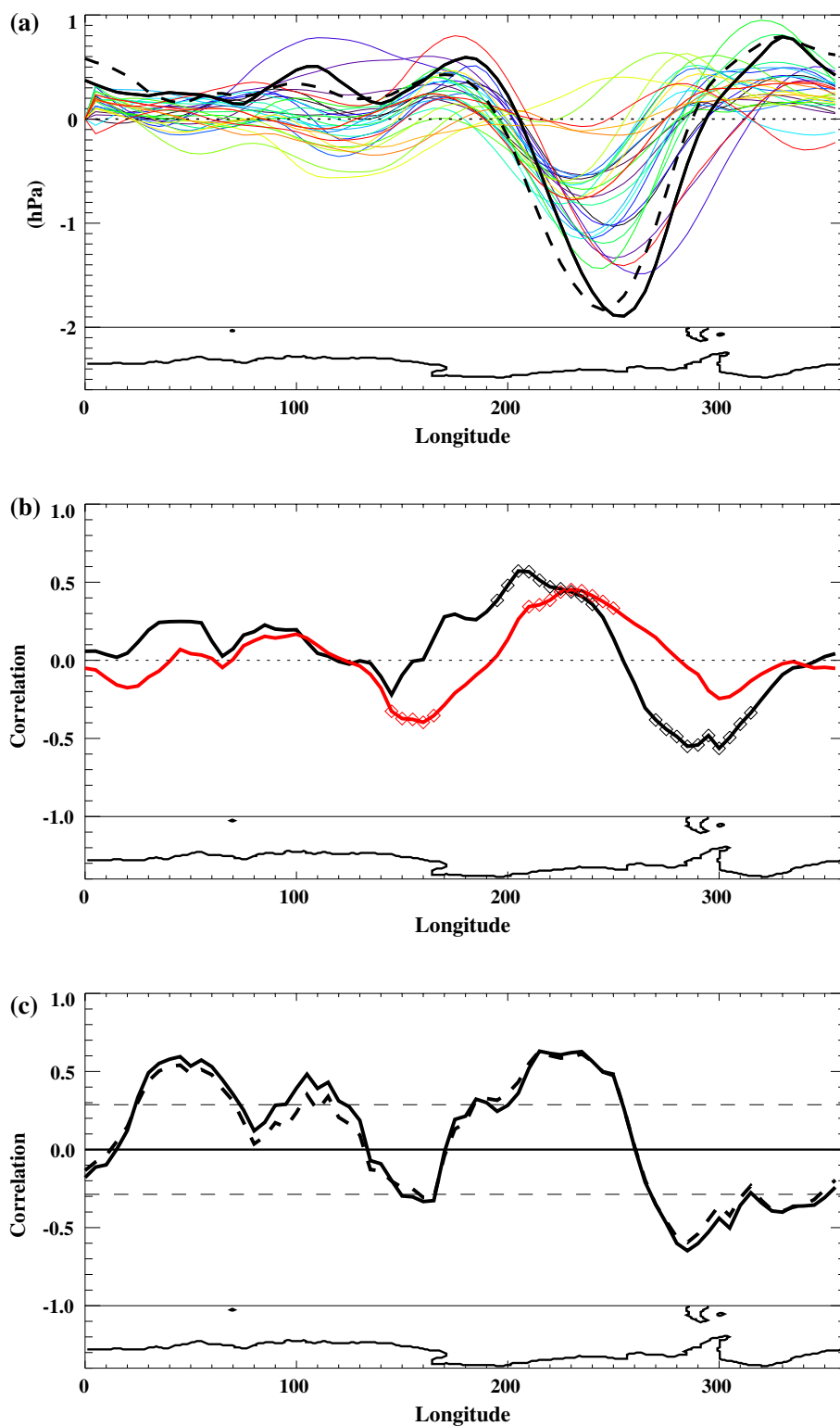


Fig. 7 The non-annular component of the annual SAM from the twentieth century reanalysis (*upper left panel*) for 1979–2012 and some select models consistent with Fig. 3. The non-annular compo-

nent is computed as the difference of the SAM-related SLP anomalies from their zonal mean. The lined contour interval is 0.5 hPa and the zero contour is not shown. The *dotted line* indicates 60S latitude

Fig. 8 **a** The SAM-associated SLP at 60S for the PI control simulations of the CMIP5 models (*colored lines*) and from the twentieth Century reanalysis (*black dash line*) and the ERA-Interim reanalysis data (Dee et al. 2011; *black line*). The reanalysis data are computed for 1979–2012. **b** The correlation of the ice area step function as a function of longitude with a metric of the non-annular component of the SAM as described in the text. Analysis is shown for the step function at 1 year lag (*black*) and 5 years lag (*red*). Values significant at the 95% level are indicated by the *diamonds*. **c** The correlation of the observed annual 1979–2012 detrended longitudinal ice area with the annual detrended SAM index obtained from the ERA-Interim reanalysis (*solid*) and the twentieth century reanalysis (*dash*). The *dashed line* indicates the 95% significance level



In response to anthropogenic forcing, the CESM-LE DJF SAM trends exhibit a discernible shift to positive values in the late twentieth century, which is consistent with the observed trend (Fig. 9a). The simulated mean trend for the

1975–2004 period is significantly different from zero at the 95% level. However, internal variability as diagnosed from the spread of trends across different ensemble members is still considerable, with a range of trends from -0.009 to

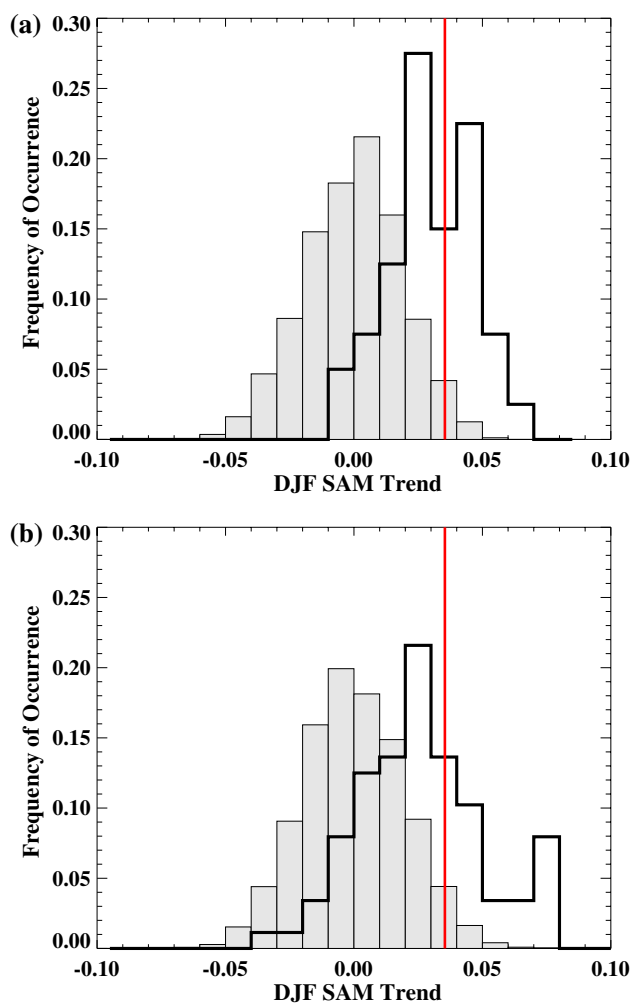


Fig. 9 The frequency of occurrence of 30 year trends in the DJF SAM timeseries from the **a** CESM-LE runs and **b** CMIP5 runs. The trends are in units of standard deviation per year. Shown are all possible trends from the pre-industrial control runs (*light grey*), trends from ensemble members for 1975–2004 (*black lines*), and the 1979–2008 trend from the observationally-based twentieth century reanalysis (Compo et al. 2011) in *red*

0.066 standard deviations per year across the members for 1975–2004. The CMIP5 models as a group also simulate a significant shift in the 30-year trends to positive values for the 1975–2004 period as compared to trends in their pre-industrial climates (Fig. 9b). The late twentieth century trend distribution is wider than the CESM-LE, with a range of -0.034 to 0.079 standard deviations per year for the 1975–2004 period. This wider spread is likely due in part to different prescribed forcing, including ozone, among the models and different model physics. However, as the comparison to CESM-LE suggests, internal variability also likely plays a large role in the variation in DJF SAM trends across the CMIP5 ensemble.

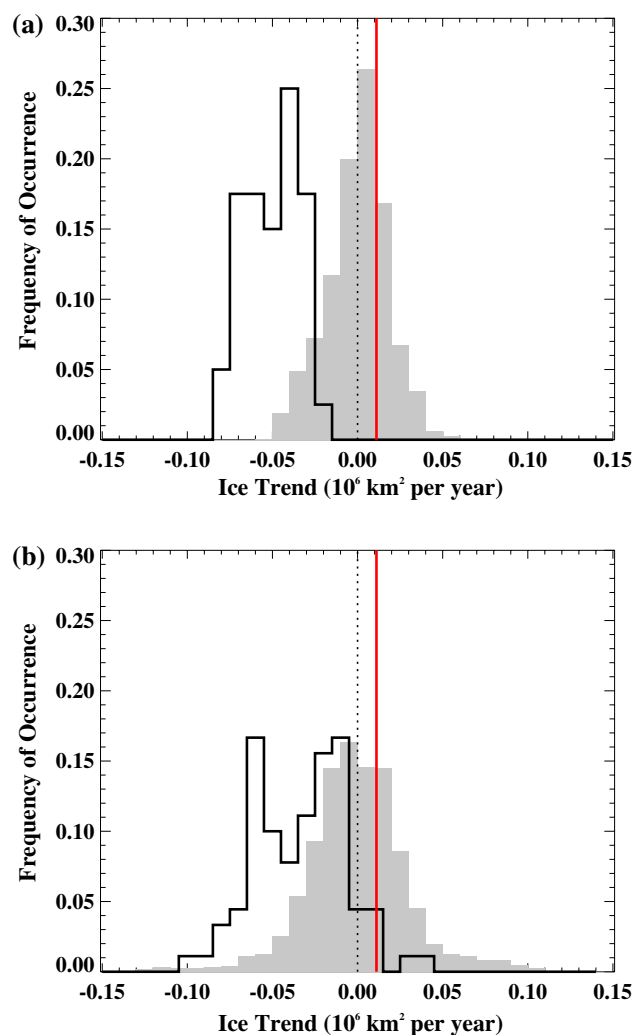
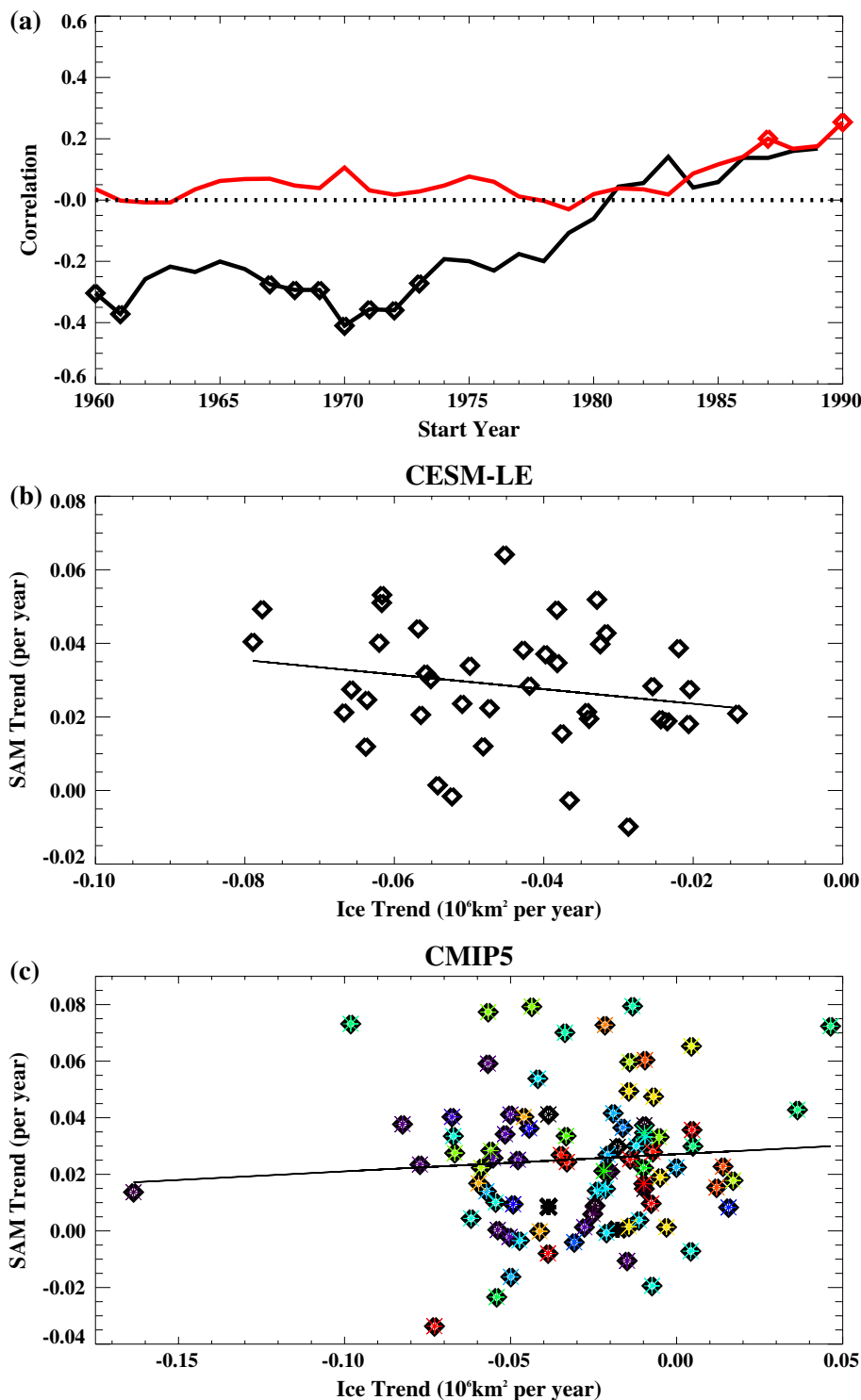


Fig. 10 Thirty year trends in annual mean total Antarctic sea ice extent from **a** the CESM-LE and **b** the CMIP5 ensemble. The ice trends are in units of 10^6 km² per year. The *grey shading* indicates the distribution of all possible 30 year trends in the pre-industrial control simulations. The *black bars* are the distribution of trends from 1975 to 2004. The *red line* shows the 1979–2008 observed trend (Fetterer et al. 2002) for reference. The *dotted line* indicates a trend of zero

The distribution of annual sea ice extent trends from the CESM-LE and CMIP5 ensembles are shown in Fig. 10. As discussed in previous studies (Mahlstein et al. 2013; Turner et al. 2013a), the scatter in twentieth century sea ice trends across the climate models is large, with most simulations (and all members of the CESM-LE) showing ice loss over the 1975–2005 time period. This is in contrast to observations, which show a small increasing trend in the total Antarctic sea ice extent over the satellite record since 1979 (e.g. Simmonds 2015). As indicated by the CESM-LE, internal variability can have a strong impact on the spread of trends from individual climate model realizations (see

Fig. 11 The **a** correlation of the annual mean sea ice trends and DJF SAM trends from the CESM-LE (*black*) and CMIP5 simulations (*red*) for different length trends. All trends run through 2005 and start at the year shown on the x-axis. **b** A scatter plot of the annual mean 1970–2005 sea ice trends relative to the DJF SAM trends in the CESM-LE. **c** Similar to panel **b** but for the CMIP5 simulations



also Polvani and Smith 2013). This likely contributes to an important fraction of the spread in sea ice extent trends among the different CMIP5 models. However, given the wider spread in trends from the CMIP5 simulations, differences in the prescribed external forcing and model structure also likely contribute.

4.2 How are the twentieth century SAM timeseries and sea ice trends related?

Figure 11 shows the correlation of DJF SAM trends and annual mean sea ice extent trends from the CESM-LE and from the CMIP5 simulations. In general, for the CESM-LE,

the spread in DJF SAM trends across the ensemble members is negatively correlated with the ice extent trends for timescales longer than about 25 years in the late twentieth century. These correlations only reach about 0.4, which is significant at the 95% level, but still quite small. Clearly other factors contribute to the spread in long-term sea ice trends across the CESM-LE members, but internal low-frequency variations in the SAM do appear to play a modest role. Members with larger DJF SAM trends tend to have enhanced ice loss in the twentieth century. This appears somewhat different from the analysis of the CMIP5 models. When the collection of CMIP5 models is considered (Fig. 11c), little correlation exists between the DJF SAM trends and sea ice extent trends. Taken at face value, this suggests little influence of the SAM on sea ice trends within the twentieth century in the models.

However, as noted in Sect. 3, the models differ considerably in the simulated response of sea ice to a SAM perturbation. We can account for this in the twentieth century simulations by convolving the twentieth century SAM timeseries with the response function obtained from the PI control runs. More specifically, we use Eq. (1) to provide an estimate of a sea ice property (SI) by multiplying the impulse response function ($G(\tau_i)$) estimated from the PI control simulations by the time-varying twentieth century DJF SAM anomalies at the appropriate time lag and summing this over the time lags. This means that the computed ice property is dependent on the prior 20 year evolution of SAM variations. This provides an estimate of the sea ice variations in the twentieth century that can be attributed to the transient DJF SAM anomalies. This analysis is performed for all twentieth century ensemble members of the CMIP5 integrations that are available (Table 2) and for all members of the CESM-LE.

Figure 12 shows the correlation of the trends in the twentieth century annual mean Antarctic sea ice extent and the trends in the SAM-related sea ice extent response obtained through the convolution analysis. When the different model responses to the SAM are accounted for, a significant relationship emerges for trends longer than about 20 years. This indicates that differences in the twentieth century transient SAM anomalies and the respective model responses to those anomalies are correlated with the spread of sea ice extent trends in the CMIP5 simulations at about $R = 0.5$. Comparing Figs. 11 and 12, the CESM-LE analysis also shows higher correlations for the convolution analysis. Given that all CESM-LE members use the same impulse response function ($G(\tau_i)$) in the convolution analysis, this suggests that the transient nature of the SAM anomalies, and not just the linear trends, are important for the simulated sea ice response.

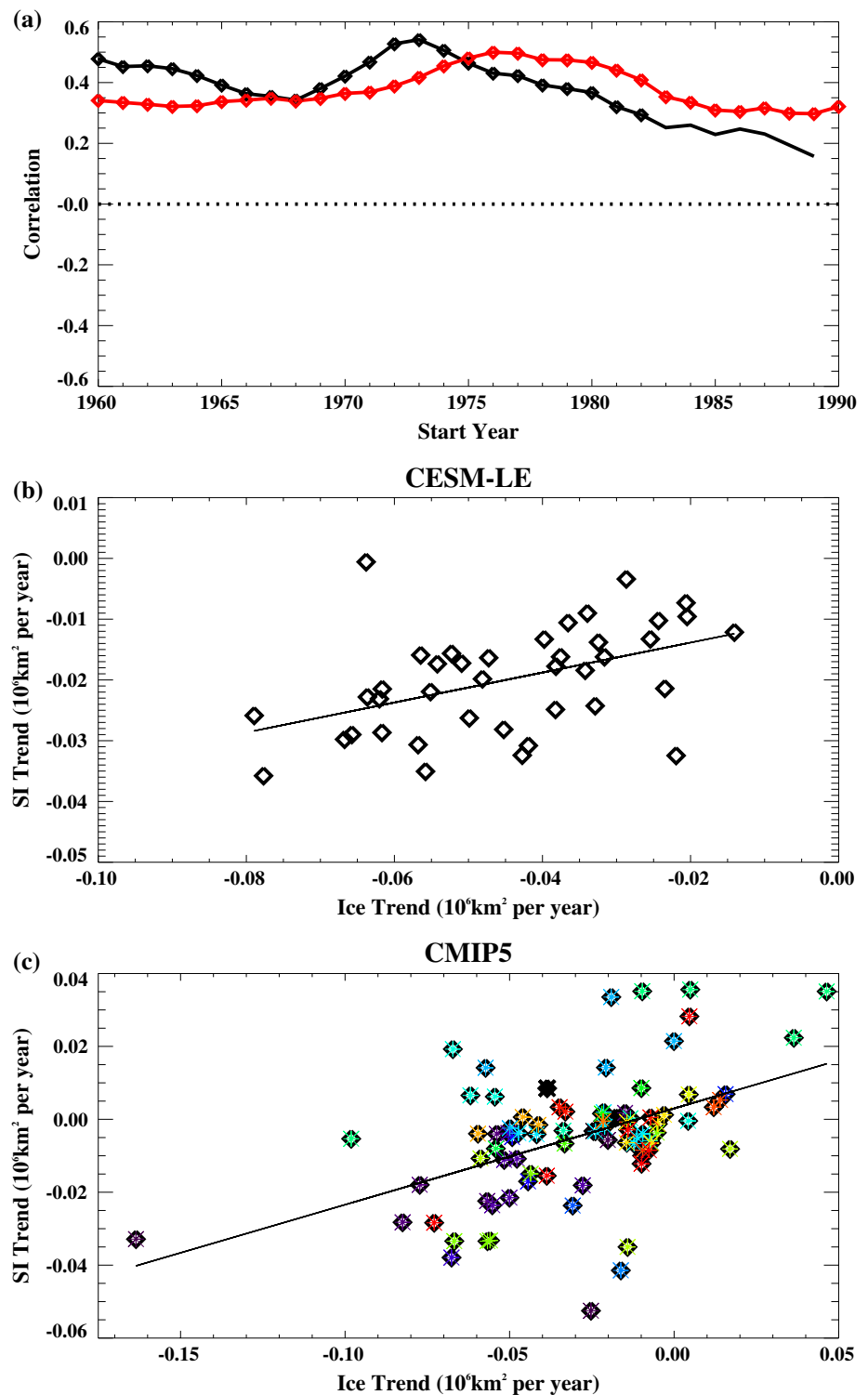
Assuming that the models simulate a realistic sea ice response to SAM variations, we should be able to obtain an

estimate of the effect of SAM variability on the observed sea ice by performing a similar convolution analysis using the modeled response function but subject to the observed SAM timeseries. This would account for both the effects of external forcings and the internal variability that occurred in the observed atmosphere. The convolution analysis approximates sea ice extent based on SAM conditions during the previous 20 years. As such, a long and consistent observationally-based SAM index is needed for this analysis (for example, to assess sea ice conditions starting in 1979, requires SAM information starting in 1960). This excludes the use of many reanalysis products because they are short in length and/or show spurious trends associated with changing data input (e.g. Bromwich et al. 2007; Swart et al. 2015). As such, we perform the analysis using a SAM index derived from the twentieth century reanalysis (Compo et al. 2011), which assimilates only surface pressure observations. Prior to the International Geophysical Year in 1957, these observations were particularly sparse in the high southern latitudes leading to larger uncertainty in the reanalysis data and so we limit our analysis to the post 1957 period. To test the influence of the observationally-based data product, we repeat the analysis using a station-based estimate of the SAM index that is available since 1957 (Marshall 2003). For the period from 1957 to 2005, the DJF SAM timeseries from these two different datasets are correlated at $R = 0.90$.

Shown in Fig. 13 is a convolution analysis using the two observationally-based estimates of the DJF SAM timeseries for both the total Antarctic sea ice extent and the longitude dependent sea ice area response. The analysis is performed using the response functions from the individual models and then averaged to obtain a multi-model mean response. This multi-model mean response indicates DJF SAM-driven ice loss in the annual mean for total ice cover trends through 2005 and for ice area at essentially all longitudes for the 1979–2005 trends. However, as indicated on the figures, the uncertainty associated with the different response functions from the models is considerable. Additional uncertainty arises from the determination of the observed SAM evolution. Comparing between the reanalysis and station-based SAM results (Fig. 13a–d), the trend in the sea ice response from 1979 to 2004 is typically larger when using the twentieth century reanalysis data. This is consistent with a larger DJF SAM trend in that data. However, this appears to be a considerably smaller source of uncertainty than the model response functions themselves.

Observed trends in sea ice are influenced by SAM-driven variations, the effects of other forcings, and internal variability. As such, a discrepancy between the observed trends and analysis shown in Fig. 13 could merely indicate the influence of non-SAM variations and may not

Fig. 12 The **a** correlation of the annual mean sea ice trends and trends in the SAM-related sea ice response obtained through a convolution analysis for the CESM-LE (*black*) and CMIP5 simulations (*red*). Correlations are computed for different length trends. All trends run through 2005 and start on the year shown on the x-axis. Significant values are indicated by the *diamonds*. **b** A scatter plot of the annual mean 1970–2005 sea ice trends and 1970–2005 trend in the SAM-related sea ice response for the CESM-LE. **c** Similar to panel **b** except for the CMIP5 simulations



necessarily indicate an issue with the models. Nevertheless, the observed trends generally are within the rather large standard deviation in the sea ice response trends from the convolution analysis. The primary exception to this is in the western Ross Sea region, where the observed trends are positive and well outside the multi-model spread. Notably,

observed ice trends within this region were also highlighted by Hobbs et al. (2015) as being outside simulated variability. This indicates that in the western Ross Sea either the model simulated response to the SAM is problematic or that other forcings are playing a strong role in the observed Ross Sea ice trends.

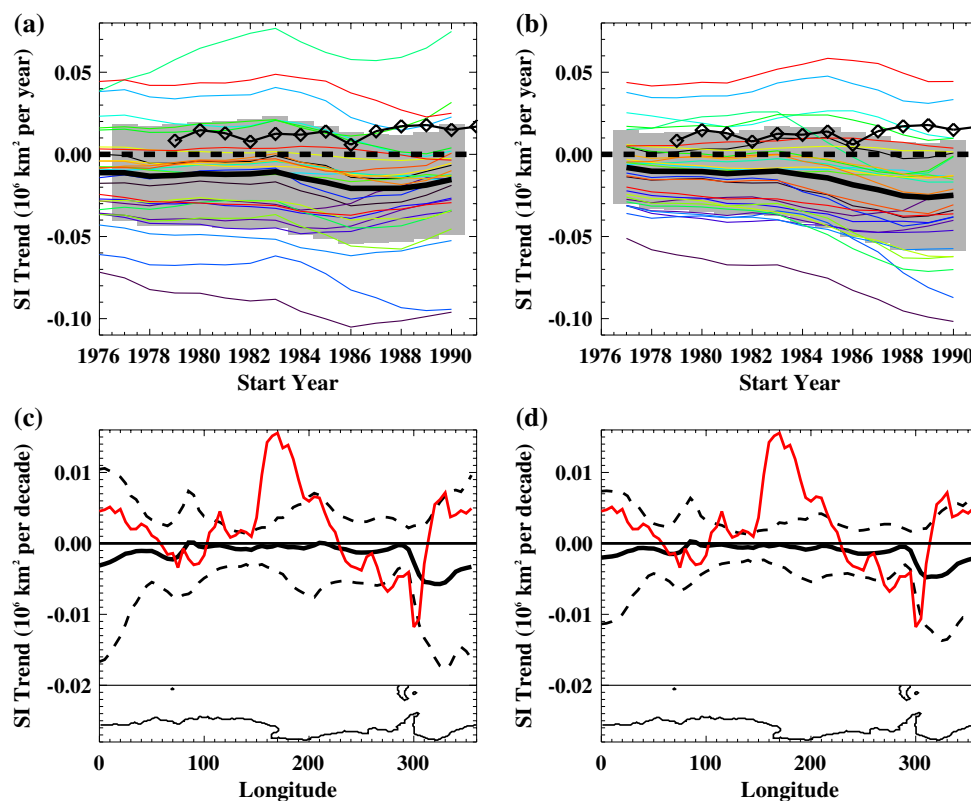


Fig. 13 Trends in the sea ice response to estimates of the observed DJF SAM as obtained through the convolution analysis. **a** Trends in the total ice extent response to the DJF SAM from the twentieth century reanalysis. Shown are values using the individual model response functions (*thin colored lines*), the multi-model mean (*thick black line*) and the standard deviation (*grey shading*). The *dashed line* shows the zero line. The *line with diamonds* shows the observed ice

extent trend. Trends run through 2004 with the start year for the trend shown on the x-axis. **b** The same as panel **a** but using the normalized station-based DJF SAM index. **c** The 1979–2004 trend in the ice area response to the DJF SAM from the twentieth century reanalysis as a function of longitude for the multi-model mean (*thick black line*), the standard deviation (*dashed line*) and the observed trend (*red line*). **d** The same as panel **c** but using the station-based DJF SAM index

5 Conclusions

The Southern Annular Mode (SAM) is the dominant mode of variability in the extratropical Southern hemisphere (e.g. Thompson and Wallace 2000) and has exhibited a positive trend in the late twentieth century largely in response to ozone loss (e.g. Marshall 2003). Both observational and modeling studies have documented that the SAM has numerous effects on the surface climate, including variability in sea ice and ocean conditions (e.g. Hall and Visbeck 2002; Lefebvre et al. 2004; Sen Gupta and England 2006; Stammerjohn et al. 2008; Sigmond and Fyfe 2010; Bitz and Polvani 2012). However, results of these studies have been seemingly at odds on whether a positive SAM leads to increased (e.g. Hall and Visbeck 2002; Sen Gupta and England 2006) or decreased (e.g. Sigmond and Fyfe 2010; Bitz and Polvani 2012) Antarctic sea ice.

If the time evolution of the sea ice response is considered, these disparate results can be reconciled (Ferreira et al. 2015). In response to a positive SAM anomaly,

increased equatorward Ekman drift results, which increases Antarctic sea ice extent. Enhanced upwelling near the continent also occurs, which brings warmer subsurface waters to the surface and contributes to enhanced warming and ice melt. As documented by Ferreira et al. (2015), the relative importance of these factors is time dependent, leading to increased sea ice extent on short timescales but decreases in the longer term. However, in this context, the definition of short and long timescales is somewhat nebulous and even for the two models analyzed by Ferreira et al. both the timescale and overall magnitude of the response differed.

Here we have characterized the response of sea ice to SAM anomalies across a large set of CMIP5 pre-industrial control simulations. This analysis indicates that climate models do typically simulate a two-timescale response with an initial increase in sea ice extent followed by an eventual decline. This is consistent with other recent studies that point to ocean warming and ice loss on the longer term (e.g. Sigmond and Fyfe 2014; Kostov et al. 2016). Our results show that the ice response is not spatially uniform

however, with the Antarctic Peninsula region exhibiting decreases and the West Pacific region increases in sea ice area at all time lags in the multi-model mean response. After about 5 years, the ice area decreases in the Peninsula region extend to the entire Weddell Sea and dominate the total ice extent response, leading to the overall ice declines. Differences across the models in the regional character of sea ice change are associated with the non-annular structure of SAM anomalies, and in particular differences across the models in how SAM variability projects onto the Amundsen Sea Low (ASL). As discussed by Hosking et al. (2013), many of the CMIP5 models simulate important biases in their depiction of the ASL, which could affect this aspect of the simulated sea ice forcing. However, while this is important for the spatial variations of the sea ice response, the resulting ice anomalies are largely compensating and so the non-annular structure of the simulated SAM has little influence on the total ice extent response. At long timescales, the Weddell Sea region dominates the across-model uncertainty in the sea ice response indicating that simulating better conditions within this region is needed.

In response to a step increase in the SAM, the majority (about 70%) of the models transition from ice gain to ice loss within 7 years. However, this varies considerably across the models, with several models transitioning within the first year and others simulating ice gain for all time lags considered (out to 20 years). The magnitude of the initial ice extent gain is significantly related to the strength of the anomalous SAM-related westerlies, indicating that adequately simulating SAM characteristics is important for the ice response. A complementary study (Kostov et al. 2016), which considers the SST relationships to SAM variations, also indicates that ocean model discrepancies are important in that different mean ocean conditions influence how effective anomalous winds are at driving ocean heat transport changes. A comparison to the Kostov et al. results suggests that these mean model biases also affect the sea ice response to the SAM. Our regional analysis indicates that biases within the Weddell Sea region may be particularly important for differences in the long timescale sea ice response across models.

The different model responses to SAM variations, as diagnosed from the pre-industrial control runs, have implications for the transient climate response in the twentieth century. For the 1975–2004 period, the CMIP5 models simulate a discernible shift to positive SAM trends in the DJF season. This is consistent with prescribed or simulated ozone loss in the models. However, there is also a large spread in the trends across different simulations, much of which may be attributable to internal variability as diagnosed from a large ensemble of simulations from a single model. A simple correlation analysis suggests little influence of the different simulated SAM trends on sea ice

extent. However, if the different model SAM responses are accounted for, a significant relationship emerges. This indicates that different simulated transient SAM variations can account for a significant fraction of the late twentieth century spread in sea ice extent trends in the models provided that the different model responses are considered.

Consideration of the modeled SAM responses acting on the observed DJF SAM timeseries suggests that variations in the observed SAM have contributed to a modest decrease in ice extent, with reductions occurring at all longitudes, during the late twentieth century. However, given the large uncertainty in the modeled response to SAM variations, the actual influence of SAM variations for twentieth century ice conditions remains unclear. Better constraints on the simulated sea ice response to the SAM are needed to more accurately simulate and understand its influence on trends in the Antarctic. As discussed by Kostov et al. (2016) biases in the mean ocean state appear to play an important role and should be the subject of future model improvements. Work also is needed to diagnose the relative importance of other climate model biases and possible missing processes on the SAM response.

Acknowledgements The authors were supported under the NSF FESD program, Grant award #1338814. Y.K. received support from an NSF MOBY Grant, award #1048926. L.L. received support from a NASA Grant, award NNX14AH74G. We acknowledge the World Climate Research Programme's Working Group on Coupled Modelling, which is responsible for CMIP, and we thank the climate modeling groups (listed in Table 1 of this paper) for producing and making available their model output. For CMIP the U.S. Department of Energy's Program for Climate Model Diagnosis and Intercomparison provides coordinating support and led development of software infrastructure in partnership with the Global Organization for Earth System Science Portals. We also thank the CESM Large Ensemble Community Project and supercomputing resources provided by NSF/CISL/Yellowstone for providing the CESM-LE simulations. We also thank Dr. Peter Gent for comments on an earlier version of this manuscript.

References

- Arblaster JM, Meehl GA (2006) Contributions of external forcings to Southern Annular Mode trends. *J Clim* 19:2896–2905
- Bitz CM, Polvani LM (2012) Antarctic climate response to stratospheric ozone depletion in a fine resolution ocean climate model. *Geophys Res Lett*. doi:[10.1029/2012GL053393](https://doi.org/10.1029/2012GL053393)
- Bromwich DH, Fogt RL, Hodges KI, Walsh JE (2007) A tropospheric assessment of the ERA-40, NCEP, and JRA-25 global reanalyses in the polar regions. *J Geophys Res*. doi:[10.1029/2006JD007859](https://doi.org/10.1029/2006JD007859)
- Cionni I, Eyring V, Lamarque JF, Randel WJ, Stevenson DS, Wu F, Bodeker GE, Shepherd TG, Shindell DT, Waugh DW (2011) Ozone database in support of CMIP5 simulations: results and corresponding radiative forcing. *Atmos Chem Phys Discuss* 11(4):10875–10933
- Comiso JC (2000, updated 2015) Bootstrap sea ice concentrations from Nimbus-7 SMMR and DMSP SSM/I-SSMIS, version 2 [1979–2005]. Boulder, Colorado USA. NASA National Snow

- and Ice Data Center Distributed Active Archive Center. doi: <http://dx.doi.org/10.5067/J6JQLS9EJ5HU>
- Compo GP et al (2011) The twentieth century reanalysis project. *Q J R Meteorol Soc* 137:1–28. doi:[10.1002/qj.776](https://doi.org/10.1002/qj.776)
- Dee DP et al (2011) The ERA-interim reanalysis: configuration and performance of the data assimilation system. *QJR Meteorol Soc* 137:553–597. doi:[10.1002/qj.828](https://doi.org/10.1002/qj.828)
- Deser C, Phillips A, Bourdette V, Teng H (2012) Uncertainty in climate change projections: the role of internal variability. *Clim Dyn* 38:527–546. doi:[10.1007/s00382-010-0977-x](https://doi.org/10.1007/s00382-010-0977-x)
- Downes SM, Hogg AM (2013) Southern Ocean circulation and eddy compensation in CMIP5 models. *J Clim* 26(18):7198–7220
- Eyring V et al (2013) Long-term ozone changes and associated climate impacts in CMIP5 simulations. *J Geophys Res Atmos* 118:5029–5060. doi:[10.1002/jgrd.50316](https://doi.org/10.1002/jgrd.50316)
- Ferreira D, Marshall J, Bitz CM, Solomon S, Plumb A (2015) Antarctic Ocean and sea ice response to ozone depletion: a two-time-scale problem. *J Clim* 28:1206–1226. doi:[10.1175/JCLI-D-14-00313.1](https://doi.org/10.1175/JCLI-D-14-00313.1)
- Fetterer F, Knowles K, Meier W, Savoie M (2002) Sea Ice Index. National Snow and Ice Data Center, Boulder. doi:[10.7265/N5QJ7F7W](https://doi.org/10.7265/N5QJ7F7W)
- Fogt RL, Wovrosh AJ, Langen RA, Simmond I (2012) The characteristic variability and connection to the underlying synoptic activity of the Amundsen-Bellinghousen Seas Low. *J Geophys Res* 117:D07111. doi:[10.1029/2011JD017337](https://doi.org/10.1029/2011JD017337)
- Hall A, Visbeck M (2002) Synchronous variability in the Southern Hemisphere atmosphere, sea ice, and ocean resulting from the Annular Mode. *J Clim* 15:3043–3057
- Hansen J et al (2007) Climate simulations for 1880–2003 with GISS modelE. *Clim Dyn* 29(7–8):661–696
- Hasselmann K, Sausen R, Maier-Reimer E, Voss R (1993) On the cold start problem in transient simulations with coupled atmosphere-ocean models. *Clim Dyn* 9:53–61. doi:[10.1007/BF00210008](https://doi.org/10.1007/BF00210008)
- Hobbs WR, Bindoff NL, Raphael MN (2015) New perspective on observed and simulated Antarctic sea ice extent trends using optimal fingerprinting techniques. *J Clim* 28:1543–1560. doi:[10.1175/JCLI-D-14-00367.1](https://doi.org/10.1175/JCLI-D-14-00367.1)
- Hosking JS, Orr A, Marshall GJ, Turner J, Phillips T (2013) The influence of the Amundsen-Bellinghousen Seas low on the climate of West Antarctic and its representation in coupled climate model simulations. *J Clim* 26:6633–6648. doi:[10.1175/JCLI-D-12-00813.1](https://doi.org/10.1175/JCLI-D-12-00813.1)
- Hurrell JW et al (2013) The community earth system model: a framework for collaborative research. *Bull Am Met Soc*. doi:[10.1175/BAMS-D-12-00121.1](https://doi.org/10.1175/BAMS-D-12-00121.1)
- Hwang YT, Frierson DMW (2013) A link between the double-intertropical convergence zone problem and cloud biases over the Southern Ocean. *Proc Natl Acad Sci* 110:4935–4940. doi:[10.1073/pnas.1213302110](https://doi.org/10.1073/pnas.1213302110)
- Kawase H, Nagashima T, Sudo K, Nozawa T (2011) Future changes in tropospheric ozone under representative concentration pathways (RCPs). *Geophys Res Lett* 38:L05801. doi:[10.1029/2010GL046402](https://doi.org/10.1029/2010GL046402)
- Kay JE et al (2015) The community earth system model (CESM) large ensemble project: a community resource for studying climate change in the presence of internal climate variability. *Bull Am Met Soc* 96:1333–1349. doi:[10.1175/BAMS-D-13-00255.1](https://doi.org/10.1175/BAMS-D-13-00255.1)
- Knutti R, Masson D, Gettelman A (2013) Climate model genealogy: generation CMIP5 and how we got there. *Geophys Res Lett* 40:1194–1199. doi:[10.1002/grl.50256](https://doi.org/10.1002/grl.50256)
- Kostov Y, Marshall J, Hausmann U, Armour KC, Ferreira D, Holland MM (2016) Fast and slow responses of Southern Ocean sea surface temperature to SAM in coupled climate models. *Clim Dyn*. doi:[10.1007/s00382-016-3162-z](https://doi.org/10.1007/s00382-016-3162-z)
- Kwok R, Comiso JC (2002) Spatial patterns of variability in Antarctic surface temperature: connections to the Southern Hemisphere Annular Mode and the southern oscillation. *Geophys Res Lett*. doi:[10.1029/2002GL015415](https://doi.org/10.1029/2002GL015415)
- Lamarque JF, Kyle GP, Meinshausen M, Riahi K, Smith SJ, van Vuuren DP, Conley AJ, Vitt F (2011) Global and regional evolution of short-lived radiatively-active gases and aerosols in the representative concentration pathways. *Clim Chang* 109:191–212
- Lefebvre W, Goosse H, Timmermann R, Fichefet T (2004) Influence of the Southern Annular Mode on the sea ice–ocean system. *J Geophys Res*. doi:[10.1029/2004JC002403](https://doi.org/10.1029/2004JC002403)
- Mahlstein I, Gent PR, Solomon S (2013) Historical Antarctic mean sea ice area, sea ice trends, and winds in CMIP5 simulations. *J Geophys Res Atmos* 118:5105–5110. doi:[10.1002/jgrd.50443](https://doi.org/10.1002/jgrd.50443)
- Marsh D, Mills M, Kinnison DE, Lamarque JF (2013) Climate change from 1850 to 2005 simulated in CESM1(WACCM). *J Clim* 26:7372–7391. doi:[10.1175/JCLI-D-12-00558.1](https://doi.org/10.1175/JCLI-D-12-00558.1)
- Marshall GJ (2003) Trends in the Southern Annular Mode from observations and reanalyses. *J Clim* 16:4134–4143. doi:[10.1175/1520-0442\(2003\)016<4134:TITSAM>2.0.CO;2](https://doi.org/10.1175/1520-0442(2003)016<4134:TITSAM>2.0.CO;2)
- Pezza AB, Rashid HA, Simmonds I (2012) Climate links and recent extremes in Antarctic sea ice, high-latitude cyclones, Southern Annular Model and ENSO. *Clim Dyn* 38:57–73. doi:[10.1007/s00382-011-1044-y](https://doi.org/10.1007/s00382-011-1044-y)
- Phillips AS, Deser C, Fasullo J (2014) A new tool for evaluating modes of variability in climate models. *EOS* 95:453–455. doi:[10.1002/2014EO490002](https://doi.org/10.1002/2014EO490002)
- Polvani LM, Smith KL (2013) Can natural variability explain observed Antarctic sea ice trends? New modeling evidence from CMIP5. *Geophys Res Lett* 40:3195–3199. doi:[10.1002/grl.50578](https://doi.org/10.1002/grl.50578)
- Previdi M, Smith KL, Polvani LM (2015) How well do the CMIP5 models simulate the Antarctic atmospheric energy budget? *J Clim* 28(20):7933–7942
- Raphael M, Holland MM (2006) Twentieth century simulation of the Southern Hemisphere in coupled models. Part I: large scale circulation variability. *Clim Dyn* 26:217–228. doi:[10.1007/s00382-005-0082-8](https://doi.org/10.1007/s00382-005-0082-8)
- Sallée JB, Shuckburgh E, Bruneau N, Meijers AJS, Bracegirdle TJ, Wang Z, Roy T (2013) Assessment of Southern Ocean water mass circulation and characteristics in CMIP5 models: historical bias and forcing response. *J Geophys Res Oceans* 118:1830–1844. doi:[10.1002/jgrc.20135](https://doi.org/10.1002/jgrc.20135)
- Schneider DP, Reusch DB (2016) Antarctic and Southern Ocean surface temperatures in CMIP5 models in the context of the surface energy budget. *J Clim* 29(5):1689–1716
- Sen Gupta A, England M (2006) Coupled ocean-atmosphere feedback in the Southern Annular Mode. *J Clim* 20:3677–3692
- Shu Q, Song Z, Qiao F (2015) Assessment of sea ice simulations in the CMIP5 models. *Cryosphere* 9(1):399–409
- Sigmond M, Fyfe JC (2010) Has the ozone hole contributed to increased Antarctic sea ice extent? *Geophys Res Lett* 37:L18502. doi:[10.1029/2010GL044301](https://doi.org/10.1029/2010GL044301)
- Sigmond M, Fyfe JC (2014) The Antarctic sea ice response to the ozone hole in climate models. *J Clim* 27:1336–1342. doi:[10.1175/JCLI-D-13-00590.1](https://doi.org/10.1175/JCLI-D-13-00590.1)
- Simmonds I (2015) Comparing and contrasting the behavior of Arctic and Antarctic sea ice over the 35 year period 1979–2013. *Ann Glaciol* 56:18–28. doi:[10.3189/2015AoG69A909](https://doi.org/10.3189/2015AoG69A909)
- Simpkins GR, Ciasto LM, Thompson DWJ, England MH (2012) Seasonal relationships between large-scale climate variability and Antarctic sea ice concentration. *J Clim* 25:5451–5469. doi:[10.1175/JCLI-D-11-00367.1](https://doi.org/10.1175/JCLI-D-11-00367.1)
- Smith KL, Polvani LM, Marsh DR (2012) Mitigation of 21st century Antarctic sea ice loss by stratospheric ozone recovery. *Geophys Res Lett* 39:L20701. doi:[10.1029/2012GL053325](https://doi.org/10.1029/2012GL053325)

- Stammerjohn SE, Martinson DG, Smith RC, Yuan X, Rind D (2008) Trends in Antarctic annual sea ice retreat and advance and their relation to El Niño–Southern Oscillation and Southern Annular Mode variability. *J Geophys Res* 108:C03S90. doi:[10.1029/2007JC004269](https://doi.org/10.1029/2007JC004269)
- Swart NC, Fyfe JC, Gillett N, Marshall GJ (2015) Comparing trends in the Southern Annular Mode and surface westerly jet. *J Clim* 28:8840–8859. doi:[10.1175/JCLI-D-15-0334.1](https://doi.org/10.1175/JCLI-D-15-0334.1)
- Szopa S et al (2013) Aerosol and ozone changes as forcing for climate evolution between 1850 and 2100. *Clim Dyn* 40:2223–2250. doi:[10.1007/s00382-012-1408-y](https://doi.org/10.1007/s00382-012-1408-y)
- Taylor KE, Stouffer RJ, Meehl GA (2012) An overview of CMIP5 and the experiment design. *Bull Am Meteor Soc* 93:485–498. doi:[10.1175/BAMS-D-11-00094.1](https://doi.org/10.1175/BAMS-D-11-00094.1)
- Thompson DWJ, Solomon S (2002) Interpretation of recent Southern Hemisphere climate change. *Science* 296(5569):895–899. doi:[10.1126/science.1069270](https://doi.org/10.1126/science.1069270)
- Thompson DWJ, Wallace JM (2000) Annular modes in the extratropical circulation. Part I: month-to-month variability. *J Clim* 13:1000–1016
- Thompson DWJ et al (2011) Signatures of the Antarctic ozone hole in Southern Hemisphere surface climate change. *Nat Geosci* 4:741–749. doi:[10.1038/ngeo1296](https://doi.org/10.1038/ngeo1296)
- Turner J, Bracegirdle TJ, Phillips T, Marshall GJ, Hosking JS (2013a) An initial assessment of Antarctic sea ice extent in the CMIP5 models. *J Clim* 26:1473–1484. doi:[10.1175/JCLI-D-12-00068.1](https://doi.org/10.1175/JCLI-D-12-00068.1)
- Turner J, Phillips T, Hosking JS, Marshall GJ, Orr A (2013b) The Amundsen Sea Low. *Int J Climatol* 33:1818–1829. doi:[10.1002/joc.3558](https://doi.org/10.1002/joc.3558)
- Turner J, Hosking JS, Bracegirdle TJ, Marshall GJ, Phillips T (2015) Recent changes in Antarctic sea ice. *Phil Trans R Soc A* 373:20140163. doi:[10.1098/rsta.2014.0163](https://doi.org/10.1098/rsta.2014.0163)
- Zunz V, Goosse H, Massonnet F (2013) How does internal variability influence the ability of CMIP5 models to reproduce the recent trend in Southern Ocean sea ice extent? *Cryosphere* 7:451–468. doi:[10.5194/tc-7-451-2013](https://doi.org/10.5194/tc-7-451-2013)